

## Interface tension in quenched QCD

Y. Iwasaki,<sup>1</sup> K. Kanaya,<sup>1</sup> Leo Kärkkäinen,<sup>2</sup> K. Rummukainen,<sup>3</sup> and T. Yoshié<sup>1</sup>

<sup>1</sup>*Institute of Physics, University of Tsukuba, Ibaraki 305, Japan*

<sup>2</sup>*Department of Physics, University of Arizona, Tucson, Arizona 85721*

<sup>3</sup>*Theory Division, CERN, CH-1211 Geneva 23, Switzerland*

(Received 13 September 1993).

We calculate the tension  $\sigma$  of the interface between the confined and deconfined phases by the histogram method in SU(3) lattice gauge theory for temporal extents of 4 and 6 using the recent high-statistics data of the QCDPAX Collaboration. The results are  $\sigma/T_c^3 = 0.0292(22)$  and  $0.0218(33)$  for  $N_t = 4$  and 6, respectively. The ratio  $\sigma/T_c^3$  shows a scaling violation similar to that already observed for the latent heat  $L$ . However, we find that the physically interesting dimensionless combinations  $(\sigma^3/L^2T)^{1/2}$  and  $\sigma T/L$  scale within the statistical errors.

PACS number(s): 12.38.Gc, 11.15.Ha, 68.10.Cr, 98.80.Cq

### I. INTRODUCTION

At the transition temperature of a first-order phase transition, a mixed state can exist where two different bulk phases are separated by an interface. The free-energy densities of the two bulk phases are equal and the free energy of the mixed state is higher than either of the pure phases by the amount  $F_s = \sigma A$ , where  $A$  is the area of the interface and  $\sigma$  is the interface tension. If the high-temperature phase transition of QCD is of first order, the interface tension between hadronic matter and the quark-gluon plasma is an important parameter for the formation of a quark-gluon plasma in heavy-ion collisions and for the nucleation of hadronic matter in the early Universe; in the latter case the inhomogeneities generated during the phase transition could affect light-element nucleosynthesis [1].

In recent years many methods have been introduced to compute numerically the interface tension in lattice SU(3) gauge theory. Because the measurement of the interface tension generally requires an extensive computing effort, so far only lattices with small temporal extents (values of  $N_t$ ) have been used. Most of the work has been concentrated on the  $N_t = 2$  system [2–4], some reaching  $N_t = 4$  [5,6].

In this work we measure the interface tension in SU(3) gauge theory with the *histogram method* introduced by Binder [7]. It requires high-statistics histograms of an order parameter at or near the phase transition point. We analyze the Polyakov loop histograms obtained by the QCDPAX Collaboration [8] with the recent high-statistics simulations on  $N_t = 4$  and  $N_t = 6$  lattices.

The dynamics of the first-order phase transition is largely governed by the latent heat  $L$  and the interface tension  $\sigma$ —the “driving” and “braking” forces of the transition. It was already observed by the QCDPAX Collaboration that the dimensionless quantity  $L/T_c^4$  does *not* scale, when  $N_t$  is increased from 4 to 6. As reported below, we observe similar behavior for the interface tension  $\sigma$ . This makes it very difficult to estimate the continuum-limit values of both  $L$  and  $\sigma$ . However, when

one studies physical processes occurring during the phase transition,  $\sigma$  and  $L$  appear in certain combinations. We find that the scaling properties of these combinations are much improved.

Let us briefly consider, as an example, the initial stage of the first-order phase transition in the early Universe. Let us assume that the system initially exists in the high-temperature phase and is cooled below  $T_c$  with a (constant) rate  $C = -\partial T/\partial t$ . According to the classical nucleation theory [9], near  $T_c$  the system spontaneously nucleates small bubbles of the low-temperature phase. The nucleation rate is  $\Gamma dt dV \propto T^4 e^{-F_B/T} dt dV$ , where  $F_B = -L\hat{T}V_B + \sigma A_B$  is the free energy of the bubble of volume  $V_B$  and area  $A_B$ , and  $\hat{T} = (T_c - T)/T_c$ . When  $T < T_c$ ,  $F_B$  has a maximum when the radius is  $R_c = 2\sigma/(L\hat{T})$ ; a bubble with this radius is called a critical bubble. The free energy of the critical bubble is given by  $F_c = F_B(R_c) = \alpha^2 \hat{T}^{-2} T_c$ , where

$$\alpha^2 = 16\pi\sigma^3/3L^2T_c. \quad (1)$$

If a bubble larger than  $R_c$  is nucleated, it starts to expand. Expanding bubbles emit shock waves which reheat the supercooled matter back close to the transition temperature, thus hindering the formation of new bubbles close to the old ones. The shock waves propagate approximately with the sound velocity  $v_s$ . New bubbles can be nucleated only in the fraction of the volume unaffected by the shock waves. This volume fraction is [1]

$$f(t) = 1 - \int_{t_c}^t dt' \frac{4}{3}\pi v_s^3 (t - t')^3 \Gamma[T(t')]. \quad (2)$$

The bubble nucleation is finished at the time  $t_{pt}$  when  $f(t_{pt}) \approx 0$ . After some algebra, the amount of supercooling and the average distance between the nucleated bubbles turn out to be

$$T_c - T_{pt} \approx \alpha\chi^{-1/2}T_c, \quad (3)$$

and

$$d \approx v_s \pi^{1/3} e^{\chi/4} \alpha\chi^{-3/2} T_c^{-1}, \quad (4)$$

respectively, where  $\chi=4\ln(T_c^2/C)$ . For the QCD phase transition in the early Universe [1],  $\chi\approx 173$ ,  $T_c\approx 150$  MeV, and  $v_s^2\approx\frac{1}{3}$ . The equations above give  $T_c-T_{pt}\approx 0.076\alpha T_c$  and  $d\approx 3\alpha a$ . The interface tension and the latent heat appear only in the combination  $\alpha$  in this case.

In Sec. II, we describe the histogram method: we briefly introduce the histogram method and apply it to the SU(3) gauge theory. Then we consider finite-size corrections to get the interface tension in the infinite-volume limit. The results are given in Sec. III and the conclusions are given in Sec. IV.

## II. THE HISTOGRAM METHOD

### A. The probability distribution

In this section we introduce the histogram method [7] and apply it to the deconfinement phase transition of SU(3) gauge theory. Let us consider SU(3) gauge theory on a lattice of size  $V\times N_t a$ , where  $V=N_x\times N_y\times N_z a^3$ , with  $a$  being the lattice spacing. On a Euclidean lattice, the temperature is given by  $T=1/(N_t a)$ . Close to the transition coupling  $\beta_c$  ( $\beta=6/g^2$ ), the probability distribution  $P(\Omega)$  of a variable  $\Omega$  that has a discontinuity at the thermodynamical limit develops a double-peak structure. For example, the order parameter  $\Omega$  can be the absolute value of the Polyakov loop. The peaks correspond to the pure phase configurations and between the peaks the dominant contributions come from mixed-state configurations where the phases are separated by interfaces. When the volume is increased, the peaks become more pronounced. The suppression of the mixed configurations is caused by the extra free energy of the interfaces.

Because of the center  $Z(3)$  symmetry of SU(3), at high temperatures there are three degenerate deconfined phases. At  $T_c$ , all of these phases and the confined phase are equally probable. This, in principle, gives rise to two different types of interfaces: interfaces between the confined phase and a deconfined phase and those between the deconfined phases. However, earlier studies [2,3] with  $N_t=2$  lattices have shown that at  $T_c$  the deconfined-deconfined interfaces are completely wet by the confined phase: effectively a layer of confined phase forms between two different deconfined phases, and  $\sigma_{\text{deconfined-deconfined}}=2\sigma_{\text{confined-deconfined}}$ . Thus, the deconfined-deconfined interfaces are strongly suppressed (a deconfined-deconfined interface is equivalent to two confined-deconfined interfaces). We also note that the histograms of the Polyakov loop in the complex plane show that the contribution from paths connecting directly deconfined phases is negligible at  $T_c$  (see footnote 13 of [8]), and the time history of the Polyakov loop indeed shows that all phase flips among different deconfined phases occur only via the confined phase. This means that the two dominant phase configurations consist of the confined phase and a deconfined phase. We therefore ignore the effect of deconfined-deconfined interfaces in the following.

With the labeling of directions such that  $N_x$  and

$N_y\leq N_z$ , the interfaces form preferentially in the  $(x-y)$  plane. For definiteness, in what follows we assume that the interfaces are oriented along the  $(x-y)$  plane; the effects of the nonfavored orientations are discussed in Sec. II B. Because of the periodic boundary conditions, there are two interfaces with a total area  $2A=2N_x N_y a^2$ .

We assume that, in large enough volumes, the distributions around the peaks are described by Gaussians:

$$c_i \exp[-(\Omega-\Omega_i)^2/d_i^2], \quad (5)$$

where  $i=1,2$  labels the two peaks, and  $d_i\propto V^{-1/2}$ ,  $c_i\propto V^{1/2}$ . Here  $\Omega_1$  and  $\Omega_2$  are the values of an extensive variable in the confined and the deconfined phases, respectively. We assume that, for the time being,  $\Omega$  is a real-valued variable. The complication which arises in the case of a complex Polyakov loop will be discussed later. The probabilities for the system to reside in the confined or deconfined phases are given by, respectively,  $\exp(-f_1 V/T)$  and  $\exp(-f_2 V/T)$ , except for a common normalization factor. Here,  $f_1$  and  $f_2$  are the free-energy densities of the confined and deconfined phases, respectively, at the given  $\beta$  and  $N_t$ : the free-energy densities of both phases can be defined by a partial partition function summed over a subset of configurations which belong to each Gaussian distribution.

We assume that in the mixed state between the peaks the two phases occupy two parts of the volumes,  $V_1$  and  $V_2$ , separated by two interfaces. The probability for the mixed phase is

$$P_m(\Omega)=c_m \exp[-(f_1 V_1+f_2 V_2)/T-\sigma 2A/T], \quad (6)$$

where  $\sigma$  is the interface tension and  $V_1+V_2=V$ .  $P_m$  depends on  $\Omega$  only through the relation

$$\Omega=(\Omega_1 V_1+\Omega_2 V_2)/V. \quad (7)$$

Then, the whole probability distribution is given by

$$P(\Omega)=P_1(\Omega)+P_2(\Omega)+P_m(\Omega), \quad (8)$$

with

$$P_i(\Omega)=c_i \exp(-f_i V/T) \exp[-(\Omega-\Omega_i)^2/d_i^2] \quad (i=1,2). \quad (9)$$

Equation (8) is our basic assumption on the distribution of the variable. The coefficients  $c$  in Eqs. (6) and (9) depend on the power of the volume  $V$ .

At the critical coupling  $\beta_c$  in the infinite-volume limit, the free-energy densities  $f_1$  and  $f_2$  are equal. On a finite lattice, however, in general  $f_1$  and  $f_2$  are not equal. When  $f_1$  and  $f_2$  are equal, the distance between the two interfaces can vary without changing the total free energy:  $P_m$  is a constant independent of  $\Omega$ . Then  $P(\Omega)$  becomes a sum of two Gaussians and a constant. On the other hand, when  $f_1$  and  $f_2$  are not equal, there is no flat part connecting the two peaks.

Let us denote the two maxima of  $P(\Omega)$  by  $p_{\max,1}$  and  $p_{\max,2}$  and the minimum between the peaks by  $p_{\min}$ . Let the minimum point be given by

$$\frac{d}{d\Omega}P(\Omega)=0, \quad (10)$$

equal to

$$\Omega=\gamma_1\Omega_1+\gamma_2\Omega_2 \quad (11)$$

with  $\gamma_1+\gamma_2=1$ , which implies  $V_1=\gamma_1V, V_2=\gamma_2V$ . Then, the leading volume dependence, that is, the  $V_i$  dependence in the exponent, cancels in the quantity

$$\hat{\sigma}_V \equiv -\frac{N_t^2}{2N_x N_y} \ln \frac{p_{\min}}{(p_{\max,1})^{\gamma_1}(p_{\max,2})^{\gamma_2}}, \quad (12)$$

which converges to the interface tension divided by  $T_c^3$  when  $V \rightarrow \infty$ :

$$\hat{\sigma} \equiv \sigma/T_c^3 = \lim_{V \rightarrow \infty} \hat{\sigma}_V. \quad (13)$$

Note that when  $p_{\max,1}=p_{\max,2}=p_{\max}$ , the denominator in the logarithm  $(p_{\max,1})^{\gamma_1}(p_{\max,2})^{\gamma_2}$  reduces to  $p_{\max}$ . The effect of the volume dependence of the coefficients  $c$  will be taken into account, when we consider finite-size corrections in the next section.

Equation (13) gives the interface tension for each  $N_t$ . To get the continuum value we still have to take the limit  $N_t \rightarrow \infty$  ( $a \rightarrow 0$ ) while keeping  $T = T_c$ .

When one applies the histogram method, one has to make some decisions which, in principle, are irrelevant in the infinite-volume limit, but can cause systematic differences when working at finite volumes. Let us first elaborate further on the choice of the variable we adopt in the analysis. Previous studies of SU(3) gauge theory on  $N_t=2$  lattices have used the action density [4] or the Polyakov loop [3,6]; we chose the latter because only the Polyakov loop gives a clear separation of phases for all the cases we have investigated.

The Polyakov loop  $\Omega$  is a complex-valued observable, and near  $\beta_c$  the distribution  $p(\Omega)$  develops four peaks, corresponding to the confined phase at the origin and three degenerate deconfined phases in the directions  $\exp(i2\pi n/3)$ ,  $n=0,1,2$ . While, in principle, one could apply Eq. (12) to a complex-valued order parameter, this would require excessive statistical quality of the data. We projected  $\Omega$  to the real axis by either using the absolute value ( $\Omega_{\text{abs}}$ ) or by rotating it ( $\Omega_{\text{rot}}$ ), by multiplying it with  $\exp(i2\pi n/3)$ , to the sector  $-\pi/3 < \arg \Omega \leq \pi/3$  and taking the real part.

The projection  $\Omega \rightarrow \Omega_{\text{abs}}$  or  $\Omega_{\text{rot}}$  causes a deformation in the probability distribution near the origin. Let us assume that, in a large enough volume, the original distribution of the peak at the origin is given by  $P(\Omega) = C \exp(-|\Omega|^2/d^2)$ , where  $C \propto V$  and  $d \propto V^{-1/2}$ . The projection changes this to

$$P(\Omega_{\text{abs}}) = Cd2\pi(\Omega_{\text{abs}}/d) \exp(-\Omega_{\text{abs}}^2/d^2), \quad (14)$$

$$P(\Omega_{\text{rot}}) = Cd3\sqrt{\pi} \operatorname{erf}(\sqrt{3}\Omega_{\text{rot}}/d) \exp(-\Omega_{\text{rot}}^2/d^2). \quad (15)$$

The maxima of these distributions are  $\sqrt{2\pi}e^{-0.5} \times Cd$  for  $P(\Omega_{\text{abs}})$  and  $3.2354\dots \times Cd$  for  $P(\Omega_{\text{rot}})$ , where  $Cd \propto V^{-1/2}$ , in accord with Eq. (5). On the other hand, the modifications in the other peaks away from the origin

should be small and can be neglected.

Now let us consider what happens for  $\hat{\sigma}_V$  in these cases. After some algebra we find that the  $\hat{\sigma}_V$  in this case also is given by Eq. (12) with minimum point Eq. (11).

The second choice concerns the value of  $\beta$  used in the analysis. Using the reweighting technique [10] we adjusted  $\beta$  so that the peaks of the histograms for  $\Omega_{\text{rot}}$  had equal height. Alternatively, one may use  $\beta$  where the ratio of the weights of the peaks is  $\frac{1}{3}$ , corresponding to one disordered and three ordered phases; for the two-dimensional  $q$ -state Potts model, this method has been shown to yield the correct infinite volume  $\beta_c$  up to exponentially suppressed corrections [11]. However, we did not apply this procedure here, because for the smallest volumes available to us, the minimum point cannot be clearly identified in order to apply Eq. (12). Further, as discussed above, we can expect that Eq. (12) is stable with respect to the changes in  $\beta$ . Indeed, we have checked that the  $\hat{\sigma}_V$ 's calculated at  $\beta_{\text{run}}$  agree with those calculated at  $\beta_0$  within the statistical errors. The final values of  $\beta_0$  used in the analysis are listed in Table I. The actual distributions of  $P_{\beta_0}(\Omega_{\text{rot}})$  are shown in Fig. 1, normalized so that  $p_{\max}=1$ .

Thirdly, we have to specify the way the heights are measured from the histograms. Because of statistical noise one should not just use the minima and maxima of

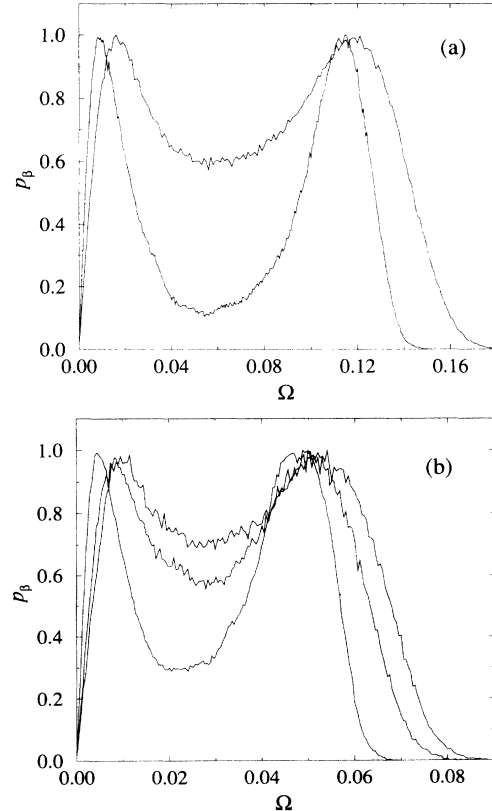


FIG. 1. Probability distributions of the rotated Polyakov loop, normalized to  $p_{\max}=1$ : (a) for  $N_t=4$  with two different volumes; (b) for  $N_t=6$  with three different volumes.

TABLE I. Parameters of the runs and the results for  $\hat{\sigma}_V$ .  $\beta_{\text{run}}$  is the value used in the actual simulation, and  $\beta_0$  is the reweighted value.  $\hat{\sigma}_V$  is calculated from Eq. (12), using both the rotated and the absolute values of the Polyakov line histograms at  $\beta_0$ .  $\gamma_1$  is measured from the  $\Omega_{\text{abs}}$  histogram at  $\beta_0$ .

$N_t$	$N_x N_y N_z$	Iterations	$\beta_{\text{run}}$	$\beta_0$	$\hat{\sigma}_V (\Omega_{\text{rot}})$	$\sigma_V (\Omega_{\text{abs}})$	$\gamma_1 (\Omega_{\text{abs}})$
4	$12^2 \times 24$	910 000	5.6915	5.691 15	0.0282(28)	0.0241(27)	0.580(37)
4	$24^2 \times 36$	712 000	5.6925	5.692 61	0.0308(17)	0.0300(16)	0.556(21)
6	$20^3$	376 000	5.8922	5.890 49	0.0146(34)	0.0123(28)	0.569(101)
6	$24^3$	480 000	5.89	5.891 97	0.0158(26)	0.0143(22)	0.547(62)
6	$36^2 \times 48$	1 112 000	5.8936	5.894 02	0.0173(25)	0.0164(26)	0.597(42)

the histograms in the analysis. To suppress random fluctuations we performed a third-order polynomial fit to the histograms near the extrema and calculated the extremum values from the fits. The fit ranges were chosen by consulting the shape of the histogram by eye; again, the results remained virtually unchanged when different ranges were used.

### B. Finite-size corrections

In this section, we discuss various finite-size corrections (FSC's) to Eq. (13). Recently there has been a lot of interest in the analysis of FSC's to the interface tension [12–14]; the analysis is particularly important here because of the different geometries of the available lattices. The starting assumptions of the analysis are that the interfaces are infinitely thin and that they do not interact with each other. We take into account the following three possible finite-size effects: Gaussian fluctuations of the order parameter in the bulk phases, Gaussian capillary-wave fluctuations of the interfaces, and the zero mode of the translation of interfaces to the direction perpendicular to the interfaces. Altogether, the ansatz becomes

$$\frac{p_{\min}}{p_{\max}} = \sum_{i=1}^3 Z_{\text{bulk}} Z_{\text{zero}} Z_{\text{CW}}^2 e^{-2N_j N_k \hat{\sigma}/N_t^2}, \quad \hat{\mathbf{i}} \perp \hat{\mathbf{j}} \perp \hat{\mathbf{k}}, \quad (16)$$

where  $i$  labels the direction perpendicular to the interfaces (of an area  $N_j N_k a^2$ ). Here,  $p_{\max}$  stands for  $(p_{\max,1})^{\gamma_1} (p_{\max,2})^{\gamma_2}$ . In the ansatz (16),  $\hat{\sigma}$  is assumed to be independent of  $N_x$ ,  $N_y$ , and  $N_z$ , but does in general depend on  $N_t$  (if we are not in the scaling region).

The bulk fluctuation term arises from the Gaussian fluctuations of the order parameter. The width of the Gaussian is proportional to  $V^{-1/2}$ , so that the normalization is  $\propto V^{1/2}$ . Because  $p_{\max}$  is in the denominator in Eq. (16),

$$Z_{\text{bulk}} \propto 1/\sqrt{N_x N_y N_z}. \quad (17)$$

The zero-mode contribution which arises from the translations of the two interfaces to direction  $z$ , keeping the relative distance  $l$  fixed, is proportional to  $N_z (\sqrt{N_x N_y})^2$ , and the contribution from the infrared divergent part of the capillary-wave fluctuation is proportional to  $(1/\sqrt{N_x N_y})^2$ . Together they give a factor

$$Z_{\text{zero}} \propto N_z^2, \quad (18)$$

an extra power of  $N_z$  originating from the measure:

$$d\Omega = (\Omega_1 - \Omega_2) N_z^{-1} dl.$$

The capillary-wave fluctuation term excluding the infrared divergent term given by Bunk [13] and Caselle, Gliozzi, and Vinti [14] is

$$Z_{\text{CW}}(N_x, N_y) \propto \left( \frac{N_x}{N_y} \right)^{1/2} [\eta(iN_y/N_x)]^{-2}, \quad (19)$$

where  $\eta$  is the Dedekind eta function:

$$\eta(\phi) = e^{2\pi i \phi/24} \prod_{n=1}^{\infty} (1 - e^{2\pi i n \phi}). \quad (20)$$

Note that  $Z_{\text{CW}}$  depends only on the ratio  $N_x/N_y$  of the interface. Not so apparent is the fact that  $Z_{\text{CW}}(N_x, N_y) = Z_{\text{CW}}(N_y, N_x)$ . Because there are two interfaces, the  $Z_{\text{CW}}$  term is squared in Eq. (16).

When deriving Eqs. (18) and (19), we have considered the interfaces in the  $z$  direction only, while in Eq. (16) we consider all interfaces including those in the  $x$  and  $y$  directions.

In our lattices the shorter spatial lengths are equal:  $N = N_x = N_y$ . Rewriting Eq. (16), we obtain the formula for  $\hat{\sigma}_V$  defined by Eq. (12):

$$\hat{\sigma}_V(N, N_z, N_t) = \hat{\sigma} - \frac{N_t^2}{N^2} \left[ c + \frac{3}{4} \ln N_z - \frac{1}{2} \ln N + \frac{1}{2} G(N, N_z, \hat{\sigma}) \right], \quad (21)$$

where  $c$  is a constant independent of  $N$  and  $N_z$  and

$$G(N, N_z, \hat{\sigma}) = \ln \left[ 1 + 2 \left[ \frac{N}{N_z} \frac{Z_{\text{CW}}(N, N_z)}{Z_{\text{CW}}(N, N)} \right]^2 \times \exp[-2(N_z - N)N\hat{\sigma}/N_t^2] \right]. \quad (22)$$

The term  $G$  appears because we have taken into account the interfaces along  $(x, z)$  and  $(y, z)$  planes and the value of it crucially depends on the geometric feature of the lattice. For example, for cubic volumes  $G = \ln 3$  and for long cylinders  $G = 0$ ; when the lattice is long ( $N_z \gg N$ ), the effect of the planar interfaces in less advantageous directions is exponentially suppressed. In our case, the effect of  $G$  is significant only for the more cubical  $N_t = 6$  lattices. Because the analytic value of  $c$  is not so far available, we perform a least-mean-squares fit of Eq. (21) to the data with parameters  $\hat{\sigma}$  and  $c$  in both the  $N_t$  cases.

Higher excitations, such as multiple-wall (4, 6, ...

walls) configurations or configurations containing a large spherical droplet of one phase embedded in the other phase, can also contribute to the probability density between the peaks. However, they have considerably larger interface area and are correspondingly more suppressed. Therefore, we neglect their effects as well as the interaction between the two interfaces.

### III. RESULTS

The parameters of the simulations are gathered in Table I. The simulations were performed with  $\beta = \beta_{\text{run}}$ . This was reweighted to  $\beta_0$  in order to obtain “equal height” histograms for  $\Omega_{\text{rot}}$  (Fig. 1). The values of  $\hat{\sigma}_V$  [Eq. (12)] for  $\Omega_{\text{rot}}$  and  $\Omega_{\text{abs}}$ , as well as the values of  $\gamma_1$  for  $\Omega_{\text{abs}}$  at  $\beta_0$ , are also presented in Table I. The error analysis was performed with the jackknife method, with bin sizes identical to those used in Ref. [8].

Let us first give the results of the interface tension in the infinite-volume limit obtained for the rotated Polyakov line:

$$\hat{\sigma}_{\text{rot}} = \sigma / T_c^3 = \begin{cases} 0.0292(22) & (N_t = 4), \\ 0.0218(33) & (N_t = 6). \end{cases} \quad (23)$$

The values of the constant  $c$  in Eq. (21) are  $-1.307(43)$  and  $-1.230(58)$  for  $N_t = 4$  and 6, respectively. For  $N_t = 6$ , the  $\chi^2$  values are quite acceptable ( $\chi^2/N_{\text{DF}} = 0.31$ ). This implies that our assumption for FSC's is reasonable.

The results obtained for the absolute value of the Polyakov line are in remarkable agreement with the values given in Eq. (23):

$$\hat{\sigma}_{\text{abs}} = \begin{cases} 0.0295(21) & (N_t = 4), \\ 0.0218(33) & (N_t = 6). \end{cases} \quad (24)$$

(For  $N_t = 6$ , the difference can be seen only in the fourth significant digit.) The values of the constant  $c$  are  $-1.267(41)$  ( $N_t = 4$ ) and  $-1.206(53)$  ( $N_t = 6$ ), and  $\chi^2/N_{\text{DF}} = 0.49$  for  $N_t = 6$ . We can conclude that the results do not depend on the choice of  $\Omega_{\text{rot}}$  or  $\Omega_{\text{abs}}$  for the order parameter. For definiteness, we use only the rotated values in the further analysis.

Let us look closer at the effects of the FSC's and, in particular, the function  $G$ . For  $N_t = 4$ , the linear fit to the data gives  $\hat{\sigma} = 0.0317(24)$  without FSC's,  $0.0301(24)$  with FSC's but with  $G = 0$ , and  $0.0292(24)$  with the full FSC ansatz—the first two values agree with the last value within the statistical errors. On the other hand, when  $N_t = 6$ , the corresponding values are  $\hat{\sigma} = 0.0185(39)$  (without FSC's),  $0.0330(39)$  ( $G = 0$ ), and  $0.0219(39)$  (full FSC ansatz). In this case the function  $G$  cancels most of the correction introduced by the other terms in Eq. (21).

The  $N_t = 4$  value above is consistent with the value  $\hat{\sigma} = 0.027(4)$  measured by Brower *et al.* [5] using a completely different method. Recently, Grossmann and Laursen [6] performed a histogram-method analysis for  $N_t = 4$  and 2 lattices, using the histograms of the  $N_t = 4$  lattices published in Refs. [8,15]. Their result [6]  $\hat{\sigma} = 0.025(4)$  is consistent with our result. (Although the

value  $\hat{\sigma} = 0.040(4)$  which originally appeared in [6] is somewhat inconsistent with our value, they recalculated it.) For  $N_t = 2$ , they obtained the value  $\hat{\sigma} = 0.092(4)$ .

The numbers above, which are listed in Table II indicate that the ratio  $\sigma/T_c^3$  does not exhibit scaling behavior for  $N_t = 2-6$ , and not even for  $N_t = 4-6$ . This makes the estimation of the continuum value of  $\sigma$  difficult.

A similar violation of scaling was also seen in the measurement of the latent heat from the same data of the QCDPAX Collaboration [8]. Because the pressure  $P$  is continuous across the phase transition, the latent heat  $L$  can be calculated from the discontinuity of  $(\epsilon - 3P)/T^4$ . On a Euclidean lattice this is proportional to the discontinuity in the average plaquette  $\langle U_{\square} \rangle$ :

$$\Delta(\epsilon - 3P)/T^4 = -72N_t^4 \tilde{\beta}(g)/g^3 \Delta \langle U_{\square} \rangle, \quad (25)$$

where  $\tilde{\beta}(g) = -a \partial g / \partial a$  is the renormalization-group beta function.  $\tilde{\beta}(g)$  can be evaluated with one- (two-)loop perturbative analysis, or, since the violation of asymptotic scaling at these  $\beta$ 's is well established, with nonperturbative Monte Carlo renormalization-group (MCRG) methods [16]. The quantity  $\epsilon - 3P$  is preferred in lattice calculations over directly measuring  $\epsilon$  or  $\epsilon + P$ , because the nonperturbative corrections to the latter quantities are not known. For  $N_t = 2$ , we use the one-loop  $\beta$  function and the plaquette gap measured by Alves, Berg, and Sanielevici [17], and for  $N_t = 4, 6$  we use the results of the QCDPAX Collaboration [8], evaluated with the one-loop  $\beta$  function and with the nonperturbative  $\beta$  function. The values are collected in Table II.

From  $L$  and  $\sigma$  we can now calculate the ratio  $\alpha^2 = 16\pi\sigma^3/(3L^2T)$ , which is also shown in Table II. We observe that, when  $N_t = 4-6$ , the scaling violations seem to be absent in  $\alpha$ , at least within the accuracy reached in this work. This holds both for the one-loop and MCRG corrected values. On the other hand, the  $N_t = 2$  value is completely off the mark when compared with the higher- $N_t$  results.

Inserting the  $N_t = 6$  value of  $\alpha_{\text{MCRG}}$  into Eqs. (3) and (4), we find that the degree of supercooling at the deconfinement phase transition in the early Universe and the average distance between the nucleation centers ( $\sim$  the scale of the inhomogeneities generated during the transition) are given by

$$(T_c - T_{\text{pt}})/T_c = 5.6(1.4) \times 10^{-4}, \quad (26)$$

TABLE II. The interface tension  $\sigma$ , the latent heat  $L = \Delta(\epsilon - 3P)$ , and the scale factor  $\alpha = [16\pi\sigma^3/(3L^2T)]^{1/2}$  for different  $N_t$ 's.  $L$  and  $\alpha$  are evaluated with the one-loop and MCRG  $\beta$  functions.

$N_t$	$\sigma/T^3$	$L_{\text{one loop}}/T^4$	$L_{\text{MCRG}}/T^4$	$\alpha_{\text{one loop}}$	$\alpha_{\text{MCRG}}$
2	0.092(4)	2.48(5)		0.046(3)	
4	0.0292(22)	4.062(85)	2.44(24)	0.0050(6)	0.0084(13)
6	0.0218(33)	2.395(63)	1.80(18)	0.0055(13)	0.0073(18)

TABLE III. The ratio of  $\sigma T/L$ , evaluated with both the one-loop and MCRG improved  $\beta$  functions.

$N_t$	$(\sigma T/L)_{\text{one loop}}$	$(\sigma T/L)_{\text{MCRG}}$
2	0.037(2)	
4	0.0072(6)	0.0120(15)
6	0.0091(14)	0.0121(22)

and

$$d = 22(5) \text{ mm} , \quad (27)$$

respectively. Another interesting quantity is the ratio  $\sigma T/L$ , which is relevant when one calculates the hydrodynamical properties of the propagating phase-transition front [18]. These values are shown in Table III. For  $N_t=4-6$ , the ratio  $\sigma T/L$  also appears to be scaling within the statistical errors.

#### IV. CONCLUSIONS

We have measured the interface tension  $\sigma$  between the confining and deconfining phases of SU(3) lattice gauge theory by the histogram method using the data from the high-statistics simulations on  $N_t=4$  and 6 lattices of the QCDPAX Collaboration [8]. The main advantage of the histogram method is that it offers a direct way to measure numerically the interface tension from order-parameter distributions. Hence, the results of ordinary finite-temperature simulations near the transition point can be used. We also made a careful analysis of finite-size corrections to the interface tension in order to estimate the infinite-volume values. We found our ansatz for finite-size corrections is quite reasonable in the sense that

our data are well fitted to the formula with quite acceptable  $\chi^2$  values.

The results,  $\sigma/T_c^3=0.0292(22)$  and  $0.0218(33)$  for  $N_t=4$  and 6, respectively, exhibit a scaling violation qualitatively similar to that for the latent heat  $L$  [8]. Since both the latent heat  $L$  and the interface tension  $\sigma$  characterize the strength of the first-order transition, it may not be surprising that we observe similar scaling violations. Thus, it is plausible that when one takes a suitable combination of  $L$  and  $\sigma$ , scaling becomes much better. Indeed, we observed that the physically relevant combinations  $\alpha^2 \propto \sigma^3 T/L^2$  and  $\sigma/LT$  scale within the statistical errors. Clearly, scaling for the dimensionless combinations and the lack of scaling for  $L$  and  $\sigma$  themselves are not satisfactory. However, we can use the combinations that do scale to predict the continuum physics.

Nevertheless, one has to be very cautious when applying these numbers to cosmology. We have neglected the effect of quarks, which may change the character of the transition completely. However, we believe that our results offer some intuition about the expected physical scales relevant for the QCD phase transition.

#### ACKNOWLEDGMENTS

We are grateful to Y. Aoki, A. Irbäck, K. Kajantie, and A. Ukawa for useful discussions. This work was partly supported by Grants-in-Aid of the Ministry of Education, Science and Culture of Japan (No. 62060001 and No. 02402003) and by the U.S. Dept. of Energy Grant No. DE-FG02-8SER40213.

- 
- [1] K. Kajantie and H. Kurki-Suonio, Phys. Rev. D **34**, 1719 (1986); G. M. Fuller, G. J. Matthews, and C. R. Alcock, *ibid.* **37**, 1380 (1987); S. Bradley *et al.*, Phys. Rev. D **43**, 1079 (1991).
- [2] K. Kajantie and L. Kärkkäinen, Phys. Lett. B **214**, 595 (1988); K. Kajantie, L. Kärkkäinen, and K. Rummukainen, Nucl. Phys. **B333**, 100 (1990); **B357**, 693 (1991); J. Potvin and C. Rebbi, Phys. Rev. Lett. **62**, 3062 (1989); S. Huang, J. Potvin, C. Rebbi, and S. Sanielevici, Phys. Rev. D **42**, 2864 (1990); **43**, 2056(E) (1991).
- [3] B. Grossmann, M. L. Laursen, T. Trappenberg, and U.-J. Wiese, Phys. Lett. B **293**, 175 (1992).
- [4] W. Janke, B. A. Berg, and M. Katoot, Nucl. Phys. **B382**, 649 (1992).
- [5] R. Brower, S. Huang, J. Potvin, and C. Rebbi, Phys. Rev. D **46**, 2703 (1992); J. Potvin and C. Rebbi, in *Lattice '90*, Proceedings of the International Symposium, Tallahassee, Florida, 1990, edited by U. M. Heller, A. D. Kennedy, and S. Sanielevici [Nucl. Phys. B (Proc. Suppl.) **20**, 317 (1991)].
- [6] B. Grossmann and M. L. Laursen, Nucl. Phys. **B408**, 637 (1993).
- [7] K. Binder, Z. Phys. B **43**, 119 (1981); Phys. Rev. A **25**, 1699 (1982).
- [8] QCDPAX Collaboration, Y. Iwasaki *et al.*, Phys. Rev. Lett. **67**, 3343 (1991); Phys. Rev. D **46**, 4657 (1992).
- [9] L. D. Landau and E. M. Lifshitz, *Statistical Physics* (Pergamon, Oxford, 1980), Pt. 1, p. 162.
- [10] I. R. McDonald and K. Singer, Discuss. Faraday Soc. **43**, 40 (1967); A. M. Ferrenberg and R. Swendsen, Phys. Rev. Lett. **61**, 2058 (1988); **63**, 1195 (1989).
- [11] C. Borgs, R. Kotecký, and S. Miracle-Solé, J. Stat. Phys. **62**, 529 (1991).
- [12] U.-J. Wiese, University of Bern Report No. BUTP-92/37 (unpublished).
- [13] B. Bunk, Int. J. Mod. Phys. C **3**, 889 (1992).
- [14] M. Caselle, F. Gliozzi, and S. Vinti, Phys. Lett. B **302**, 74 (1993).
- [15] M. Fukugita, M. Okawa, and U. Ukawa, Phys. Rev. Lett. **63**, 1768 (1989); Nucl. Phys. **B337**, 181 (1989).
- [16] J. Hoek, Nucl. Phys. **B339**, 732 (1990); J. Engels, J. Fingberg, F. Karsch, D. Miller, and M. Weber, Phys. Lett. B **252**, 625 (1990).
- [17] N. Alves, B. Berg, and S. Sanielevici, Nucl. Phys. **B376**, 218 (1992).
- [18] K. Kajantie, Phys. Lett. B **284**, 331 (1992); P. Huet, K. Kajantie, B.-H. Liu, G. Leigh, and L. McLerran, Phys. Rev. D **48**, 2477 (1993).